

Multi-Class Glioma Classification using Dual-Path Convolutional Neural Networks on MRI and Pathological Images

*B.Tech Project report submitted in partial fulfilment of the requirements
for the degree of B.Tech. in Computer Engineering*

by

Bhaskara Teja Atluri
(Roll No: COE16B004)

Under the guidance of
Dr. Umarani Jayaraman



DEPARTMENT OF COMPUTER ENGINEERING
INDIAN INSTITUTE OF INFORMATION TECHNOLOGY,
DESIGN AND MANUFACTURING, KANCHEEPURAM

May 2020

Certificate

I, **Bhaskara Teja Atluri**, with Roll No: **COE16B004** hereby declare that the material presented in the Project Report titled "**Multi-Class Glioma Classification using Dual-Path Convolutional Neural Networks on MRI and Pathological Images**" represents original work carried out by me in the **Department of Computer Engineering** at the **Indian Institute of Information Technology, Design and Manufacturing, Kancheepuram** during the period **January 2020–May 2020**. With my signature, I certify that:

- I have not manipulated any of the data or results.
- I have not committed any plagiarism of intellectual property. I have clearly indicated and referenced the contributions of others.
- I have explicitly acknowledged all collaborative research and discussions.
- I have understood that any false claim will result in severe disciplinary action.
- I have understood that the work may be screened for any form of academic misconduct.

Date: May 20, 2020

Student's Signature



In my capacity as supervisor of the above-mentioned work, I certify that the work presented in this Report is carried out under my supervision, and is worthy of consideration for the requirements of project work during the period January 2020 to May 2020.

Advisor's Name:

Advisor's Signature

Dr. Umarani Jayaraman

Assistant Professor

Computer Engineering

Abstract

Glioma is a prevalent and deadly form of brain tumor. MRI images and histopathological images are used to classify glioma and it's sub-types. For a patient's evaluation and recovery plans, classification is important. Classification done manually is costly, burdensome and prone to human errors. Thus, an automated system has been developed with convolutional neural network using conv3D layers to classify gliomas into three types namely, Astrocytoma, Oligodendrogloma and Glioblastoma from MRI modalities and pathological images. The importance of segmentation and the usage of additional imaging modalities has also been studied. The models have been trained on CPM-RadPath2019 dataset. The dual-path model which has been trained on both MRI and pathology images achieved an accuracy of 77.73% which was higher classification accuracy than the other models that were implemented. Additionally to study the role of necrosis regions in Glioblastoma classification, a binary classification between Glioblastoma and non-Glioblastoma classes has been performed with T1ce MRI modality as input to the proposed 3D CNN model. Necrosis regions appear as hyper-intense values in T1ce MRI modality. This model trained with segmented T1ce MRI modality achieved an accuracy of 89.2%.

Acknowledgements

I would extend my sincerest gratitude to **IIITDM Kancheepuram** for giving me an opportunity to carry out my project of my interest.

I would like to thank **Dr. J. Umarani** for always being an extremely supporting guide and helping out to complete the project within the stipulated amount of time through her valuable knowledge in the area. I would also thank Mr. Subin Sahayam for the great mentor he has been to be throughout this period.

I would also thank my friends who made the learning part interesting and fascinating with whose help i learned a lot during this period.

Contents

Certificate	i
Abstract	ii
Acknowledgements	iii
Contents	iv
List of Figures	vi
List of Tables	vii
1 Introduction	1
1.1 Motivation	3
1.2 Objectives	3
1.3 Structure of Thesis	3
2 Literature Review	5
2.1 Segmentation	5
2.2 Brain Tumor Segmentation Using Convolutional Neural Networks in MRI Images	5
2.2.1 Dataset	6
2.2.2 Convolution Neural Network	6
2.3 Classification	7
2.4 Deep Learning and Multi-Sensor Fusion of Glioma Classification using Multistream 2D Convolutional Networks	8
2.4.1 Dataset	9
3 Proposed Method	12
3.1 Pre-Processing	12
3.2 Segmentation	13
3.3 Convolutional Neural Network	14
4 Experimental Results	16

4.1	Dataset	16
4.2	Work Done and Results	17
4.2.1	Segmentation	17
4.2.2	3-Class Classification on MRI images	19
4.2.3	Binary Classification on MRI images	21
5	Conclusion	23
Bibliography		24

List of Figures

1.1	A)Age 0-14 years, B)Age 15-39 years, C)Age 40+ years	1
1.2	Distribution of brain and central nervous system. Note: Percentages may not add up to 100% due to rounding.	2
3.1	The flow diagram of the proposed model. Here, A - Astrocytoma, O - Oligodendrogioma and G - Glioblastoma	13
3.2	The proposed 3D convolutional neural network(CNN) architecture where the input layers consists of t1, t2, t1ce and flair images along with pathalogical images and the output layer consists of 3 neurons for each target class - Astrocytoma, Oligodendrogioma and Glioblastoma.	14
4.1	MRI modalities, i)FLAIR, ii)T1, iii)T1ce, and iv)T2	17
4.2	Few patches cropped from the brain tissue image.	17
4.3	The tumor was segmented with a dice-coefficient of 0.6023	18
4.4	All the four modalities mask with the segmented tumor region.	19
4.5	The proposed 3D convolutional neural network(CNN) architecture where the input layers consists of t1, t2, t1ce and flair images and the output layer consists of 3 neurons for each target class - Astrocytoma, Oligodendrogioma and Glioblastoma.	20
4.6	Accuracy of the proposed model on segmented and non-segmented MRI modalities(T1, T2, T1ce and FLAIR)	21

List of Tables

2.1	Hyperparameter of the proposed method	7
2.2	Overview on various types of tumor classification problems in the literature.	9
2.3	Description of Dataset-A and Dataset-B	10
2.4	Proposed architecture of the multi-stream CNN	10
2.5	Hyper-parameters of the model	11
2.6	Comparisons of classification performance	11
3.1	Caption	15
4.1	Importance of masked segmented MRI images.	19
4.2	Confusion Matrix for Glioblastoma vs Non-Glioblastoma, with and without segmentation	22
4.3	Validation accuracy from various models with different inputs	22

Chapter 1

Introduction

Glia cells support neurons and have various structural and functional roles throughout the nervous system [1]. Astrocytes, ependymocytes, oligodendrocytes, microglia, and schwann cells are the main types of glial cells in the brain among others [2]. A brain tumor is the uncontrolled growth of brain cells. The study of glioma is of paramount importance because it is the most frequently occurring malignancy among humans. A survey conducted by Ostrom et al.[3] shows that Brain and CNS tumors are the most abundant cancer locations in children aged 0-14 years. The cells called glial are the root

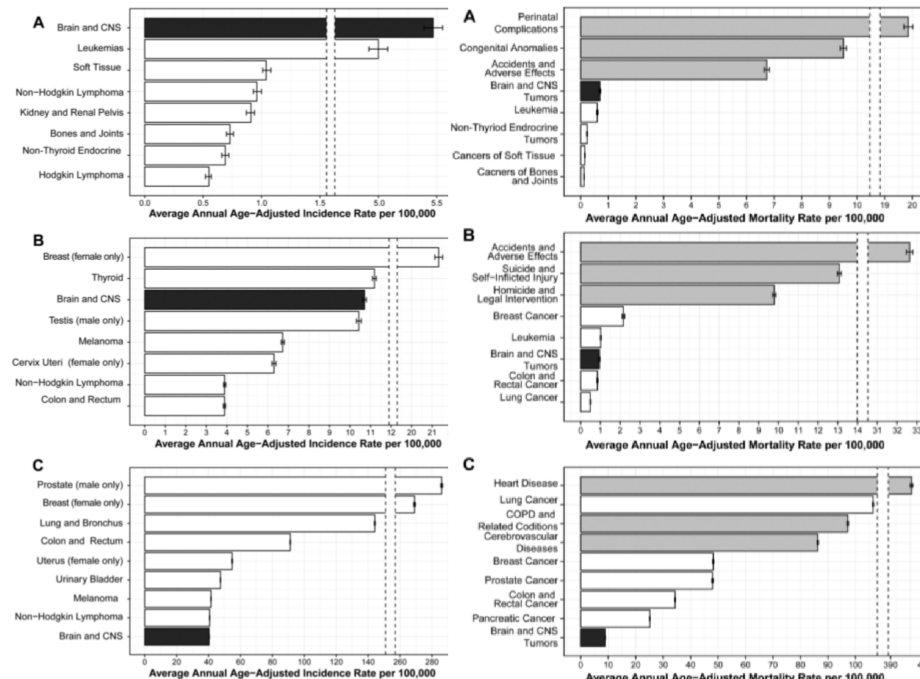


FIGURE 1.1: A)Age 0-14 years, B)Age 15-39 years, C)Age 40+ years

cause of glioma which is a prevalent and deadly form of brain tumor [3]. Benign and malignant are the types into which the brain tumors are generally grouped into. According to the World Health Organization (WHO), the tumors related to brain, and CNS are classified based on the glial cell from which the tumor is originated and they are categorized into ependymoma, oligodendrogloma, oligoastrocytoma, astrocytoma and glioblastoma. Glioblastoma is a glioma for which the origin is not known [4].

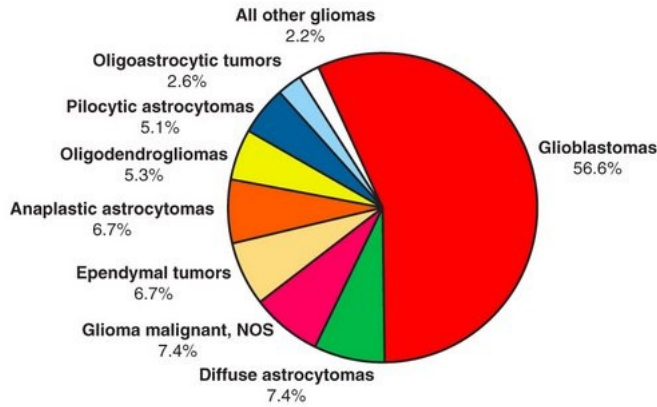


FIGURE 1.2: Distribution of brain and central nervous system. **Note:** Percentages may not add up to 100% due to rounding.

Magnetic Resonance Images(MRI), Pathological images, Ultrasound, and computed Tomography are used for identification and diagnosis of the tumor. Generally, MRI are commonly used for the diagnosis of the tumor. The four types of MRI images, namely, T2 Fluid-attenuated inversion recovery(T2-FLAIR), T1-weighted, Contrast Enhanced T1, and T2-weighted, help in identification and diagnosis, and also by studying the tumorous tissues under a microscope or by molecular testing. The diagnosis and classification has a prominent part in treatment planning. The diagnosis task is tedious, burdensome, not affordable and has a high chance of human errors [4]. So, there is a need for accurate, robust and automated system for classification, which can improve the efficiency of tumor classification and diagnosis.

Medical image processes has been an effective method for diagnosis of tumors for a long time. Several techniques such as Support Vector Machines(SVM), Boltzmann, fuzzy-C mean, random forests and neural networks are quite efficient in image processing. Feedforward Neural Network(FNN), Artificial Neural Network(ANN), Convolutional Neural Network(CNN), Probabilistic Neural Network(PNN) and Recurrent Neural Network(RNN) have all shown significant results in image processing.

But in recent times, the Convolutional Neural Networks are proven to be more efficient than others in brain tumor segmentation [5] and brain tumor classification [6].

1.1 Motivation

Brain cancer is a fatal and complex disease. Brain tumors are graded and diagnosed traditionally by pathologists, who examine the tissue sections present on glass slides under a light microscope. It is not scalable to translate clinical research studies when this process is continued to be widely applied on clinical settings, as it involves hundreds or thousands of tissue specimens. Computer-aided classification has the potential to improve brain tumor grading and diagnosis process, and also enables quantitative studies of the mechanisms of the underlying disease onset and progression.

1.2 Objectives

This work majorly focuses on developing an robust and automated system, that can classify the given tumor based on MRI and pathological images with high efficiency, thereby playing a vital role in treatment-planning. Achieving the following objectives, helps in developing an efficient and robust system.

- The importance of segmentation of the MRI images in the classification of the tumor.
- Analysis various algorithms and comparing their efficiency against each other.
- Effectively classifying the tumor into 3-Class - Glioblastoma, Astrocytoma and Oligodendrogioma.
- 2-Class Classification - (Glioblastoma, Non-Glioblastoma)
- 2-Class vs 3-Class Classification.

1.3 Structure of Thesis

The report is organized as follows. Chapter 2 gives an idea of all the existing algorithms which are developed for segmenting the MRI images, performing classification on MRI and

pathological images. Chapter 3 gives the detailed information on the proposed algorithm dual path residual neural network which is developed for classifying the tumor with MRI and pathological images as input. Chapter 4 discusses various results and compares the results of the algorithms with the proposed system. We conclude in Chapter 5, along with ideas which help in taking the proposed model to higher efficiency.

Chapter 2

Literature Review

2.1 Segmentation

Many ways are considered for directly creating a parametric or non-parametric probabilistic model for the underlying data in the process of segmenting the brain tumor. Tumors are considered being abnormalities and subjected to shape and connectivity constraints can be wedged as out-liners of regular tissue [7]. Zikic et al. [8] used a shallow CNN with two convolutional layers with probabilistic atlases accompanied by max-pooling with stride 3, and a softmax layer. According to Rao et al. [9], the outputs of an FC layer are concatenated with each softmax of the CNN and used to train a random Forest classifier, and the patch was extracted on each plane of each voxel and trained a CNN on each MRI series.

2.2 Brain Tumor Segmentation Using Convolutional Neural Networks in MRI Images

Gliomas are the most trivial and aggressive, among brain tumors, resulting in shortening the mortality rate in their malignant grade. These tumors are largely assessed usually by Magnetic Resonance Imaging(MRI), but the huge chunks of information generated by MRI will be very hard to study and thus manual segmentation on the tumor will be time-taking. Basing on Convolutional Neural networks, the segmentation process was made autonomous by exploring 3x3 kernels has been developed, with these smaller kernels having a positive

effect on over-fitting due to the lesser number of weights in the network. This model was submitted to Challenge Brats 2015.

2.2.1 Dataset

This method was trained and validated on BRATS 2015 database [10]. There are 4 modalities of MRI images for which the skulls are stripped off and are oriented along the T1ce modality. The images of each subject were already aligned with T1ce and skull stripped. 54 lower-grade gliomas along with 220 MRI images of higher grade gliomas are present, respectively in the training data of BRATS-2015 [10]. And there exists a manually segmented ground truth that identifies four types of intra-tumoral classes: necrosis, edema, non-enhancing, and enhancing tumor.

2.2.2 Convolution Neural Network

- **Initialization:** Xavier intialization is used to achieve convergence. To prevent back-propagated gradients from vanishing, the gradients are maintained in control levels.
- **Activation Function:** Rectifier Linear units(ReLU) take the responsibility for transforming the data non-linearly. We introduce a small negative slope on the negative part of the function, which is defined as

$$f(x) = \max(0, x) + \alpha \min(0, x)$$

where α is the leakyness parameter. In the last FC layer, we use softmax function.

- **Pooling:** This combines the spatially nearby features in the feature maps. We add a Max-Pooling layer after every 3 convolutional layers. Each Max-Pool layer has a 3x3 filter and stride 3.
- **Regularization:** It is used to reduce over-fitting. Dropout is used in the FC layers. It forces all the nodes of the FC layers to learn better representations and prevents from co-adapting each other.
- **Data Augmentation:** Since the class of the patch is obtained by the central voxel, the data augmentation was restricted to rotating operations. New patches are developed by rotating the original patches at angles mutiple of 90° .

Stage	Hyperparameter	Value
Initialization	bias	0.1
	weights	Xavier
Leaky ReLU	α	0.333
Dropout	p - HGG	0.1
	p - LGG	0.5
Training	epochs - HGG	20
	epochs - LGG	25
	v	0.9
	Initial ϵ	0.003
	Final ϵ	0.00003
	Batch	128
Post-processing	$\tau_{VOL - HGG}$	10000
	$\tau_{VOL - LGG}$	3000

TABLE 2.1: Hyperparameter of the proposed method

- **Loss Function:** Categorical Cross-entropy was used as the loss function, which is minimized during training.

$$H = - \sum_{j \in voxels} \sum_{k \in classes} c_{j,k} \log(\hat{c}_j, k)$$

All hyperparameters depicted in 2.1 are parameterized based on one subject in both higher and lower grade gliomas during the validation period. Edema, enhancing tumor, regular tissue, necrosis, and non-enhancing tumor are the 5 classes that are categorized by the multi-class classification model developed by the system. The model was validated on BRATS 2013 and got a dice-coefficient of 0.88 for the complete tumor segmentation. This model was placed second in the BRATS 2015 Challenge [10] achieving a dice similarity of 0.78, 0.65, and 0.75 for the complete, core, and enhancing regions, respectively.

2.3 Classification

Several brain tumor classification problems have been worked on in the past by several authors. In [11, 12, 13], the authors have tested their proposed models on 3064 selective slices of T1ce MRI modality to perform ternary classification namely, 708 meningioma, 1426 glioma, and 930 pituitary glands. Cheng et al.[12] explored various data augmentation and partitioning preprocessing methods for classification and studied their performance on Support Vector Machines(SVM), a Sparse representation-based classifier(SRC) and k-nearest neighbor (KNN) based classifier. They showed that SVM performed better after

performing data augmentation and partitioning. Ge et al.[6] implemented a 2D deep convolutional neural network for glioma classification. They tested their method on high and low-grade glioma and also glioma with and without 1p19q codeletion datasets. The input for their method used 2D slices from the MRI images in the respective datasets. Ge et al.[14] also proposed a non-invasive classification to classify IDH mutant and IDH wildtype classes from MRI images. They used a pairwise generative adversarial network(GAN) to perform the classification task on 2D MRI slices. Table 2.2 gives an overview of brain tumor classification problems available in the literature.

All methods discussed in the literature used 2D slices from MRI modalities. 2D slices capture neighborhood information but not temporal information between each continuous frames. This latter information can be useful for better tumor classification. Also, the methods explored using the Nanfang Hospital [12] dataset consist of only a T1-weighted contrast-enhanced(T1ce) MRI modality. There is no study on the performance of methods when using additional MRI modalities like T1-weighted, T2-weighted, and FLAIR. According to [10], the necrosis region is well observed in the T1ce MRI modality. Glioblastoma generally shows such necrosis regions. Based on the mentioned information, the contribution of this paper is a) propose a 3D convolution neural network to incorporate temporal information of MRI modalities, b) compare the performance of 3D CNN with 2D CNN which takes 2D slices from the 3D MRI as input, c) Study the performance of the model using a single MRI modality(T1ce) vs four MRI modalities(T1, T2, T1ce & FLAIR), d) Study the classification of Glioblastoma from T1ce MRI modality and e) provide evidence supporting the literature that segmentation before classification gives better accuracy.

2.4 Deep Learning and Multi-Sensor Fusion of Glioma Classification using Multistream 2D Convolutional Networks

Different types of scanners like enanced T1, T2, and FLAIR show different constraint and are sensitive to different brain tissues and fluid regions. The proposed multistream deep Convolutional Neural Network extracts and fuses the features from multiple sensors for glioma tumor grading. Two datasets were used for the experiments, one for classifying low/high grade gliomas, another is for classifying glioma with/without 1p19q codeletion.

Year	Paper Title	Dataset	Target Classes
2015	Enhanced Performance of Brain Tumor Classification via Tumor Region Augmentation and Partition	Public [12]	Meningioma, Glioma, Pituitary Tumor
2018	Brain Tumor Type Classification via Capsule Networks	Public [12]	Meningioma, Glioma, Pituitary Tumor
2018	Multi-grade Brain Tumor Classification using Deep CNN with Extensive Data Augmentation	Public [12]	Meningioma, Glioma, Pituitary Tumor
		Radiopaedia [11]	Grade i,ii, iii,iv
2019	Deep Learning and Multi-Sensor Fusion for Glioma Classification using Multistream 2D Convolutional Networks	BraTS2017 [15, 16]	High and Low Grade Glioma
		Mayo Clinic [17]	1p19q with and without codeletion
2019	Cross-Modality Augmentation of Brain MRI images using a Novel Pairwise Generative Adversarial Network for Enhanced Glioma Classification	TCGA [18, 19]	IDH - Mutation, IDH - wildtype
	Proposed Method	CPM-RadPath [20]	Astrocytoma, Oligodendrogioma, Glioblastoma

TABLE 2.2: Overview on various types of tumor classification problems in the literature.

The proposed model showed significant results with an accuracy of 90.87% for high/low grade glioma classification and 89.39 for with/without 1p19q codeletion.

2.4.1 Dataset

Dataset-A contains 3D brain volume images including low grade glioma(LGG) and high grade glioma(HGG) from the MICCAI BraTS 2017 [cite](#). Each patient is associated with four types of MRI modalities, namely, T1-weighted, contrast-enhanced T1, T2-weighted and T2-FLAIR. Dataset-B contains 3D MRI images from Mayo Clinic, USA, including 2 sub-categories of low grade gliomas with/without 1p19q codeletion [cite](#). Each patient is associated with two types of MRI modalities, contrast-enhanced T1, and T2-weighted. Detailed information of the two datasets are given in Table 2.3.

Class	#subjects	# T1	# T2	# FLAIR	With/without 1p19q	#subjects	# T1	# T2
HGG	210	210	210	210	with 1p19q	102	102	102
LGG	75	75	75	75	without 1p19q	57	57	

TABLE 2.3: Description of Dataset-A and Dataset-B

The architecture of the proposed model and fusion network scheme is depicted in Table 2.4. It consists of 3 streams followed by a bi-linear layer and 3 fully connected layers dedicated for the dedicated glioma classification. Each stream contains a 7-layered 2D CNN. BN stands for Batch Normalization and ReLU is Rectified Linear Unit are the terms used in 2.4. The slice of each 2D brain slices are 128*128 pixels. The last 3 fully connected layers are used for building the classifier, and the labels are obtained as the output of the last layer.

Layer	Filters	Output Size
Conv-1+Maxpool+BN+ReLU	3*3*64	64*64*64
Conv-2+BN+ReLU	3*3*128	64*64*128
Conv-3+Maxpool+BN+ReLU	3*3*128	32*32*128
Conv-4+BN+ReLU	3*3*256	32*32*256
Conv-5+Maxpool+BN+ReLU	3*3*256	16*16*256
Conv-6+BN+ReLU	3*3*512	16*16*512
Conv-7+Maxpool+BN+ReLU	3*3*512	8*8*512
Aggregation	-	8*8*512
Bilinear processing+BN	-	512*512
FC-1	256	256
FC-2	256	256
FC-3+softmax	2	2

TABLE 2.4: Proposed architecture of the multi-stream CNN

For each CNN stream, a 7-layer CNN is selected for the extraction of features from one of the sensors, after careful selection through numerous empirical tests, since stacking multiple small kernels like 3*3 increases the depth of the network and thus is better at learning more complex features. The fusion of features from 3 sensors consists of two layers of processing, aggregation and bi-linear processing. To obtain the compact feature representation the aggregation layer is used. For the modeling interactions of features from each other at different spatial locations, the bi-linear layer is utilized. Two fully connected layers with ReLU activation function which are succeeded by a fully connected layer with softmax activation function, together form the classifier. The hyper-parameters of the model are described in the table 2.5

Stage	Value
Initial weights	Xavier uniform
Initial bias	0
Adagrad optimizer	0.0001
Dropout	0.5
ReLU	0.333
L2 regularization	0.0001
epochs	50
batchsize	128

TABLE 2.5: Hyper-parameters of the model

This model has been developed for glioma classification and validated on BraTS dataset. We conjecture that overfitting in learning can be avoided using 2D slices of brain MRI and augmentation of the slice images. The model has achieved an accuracy of 90.87% for high/low grade glioma classification. Glioma classification with/without 1p19q codeletion was predicted by the model with an accuracy of 89.39%. Table 2.6 shows the results from of individual sensors as inputs along with the sensor fusion, which has the higher accuracy.

	Overall acc.	HGG acc.	LGG acc.
Enhanced T1	83.73%	84.92%	82.54%
T2-weighted	69.84%	80.15%	59.52%
FLAIR	75.40%	74.60%	76.19%
3-Sensor Fusion	90.87%	91.27%	90.48%

TABLE 2.6: Comparisions of classification performance

Chapter 3

Proposed Method

The proposed method consists of a training phase and a testing phase. The model consists of a dual path, in which each path is given MRI images and pathological images respectively. The model which takes MRI images as inputs have three stages namely, i)Pre-Processing, ii)Segmentation and, iii)Classification, while the model which takes Pathological images as input has similar stages one and three but the second stage comprises of feature extraction. The flow diagram on the proposed dual-path model is shown in figure 3.1.

3.1 Pre-Processing

The mean and standard deviation of intensity values in an MRI modality varies based on several factors like the usage of different acquisition scanners, varying imaging protocols, magnetic field strength, bias field distortion, and many more.

So, the mean (M_o) of each MRI modality (I_o) has been normalized to zero. Further, to normalize the distribution of intensities across MRI images, the voxels in zero-mean images have been divided by the standard deviation Sd_o of the original image. The resultant normalized image is denoted as I_n . The normalization is given by,

$$\text{NormalisedImage}I_n = \frac{I_o - M_o}{Sd_o}$$

The pathological images are given as digitized whole slide tissue images. Since these are very high-resolution .tiff images, it is feasible to train the model with these images as

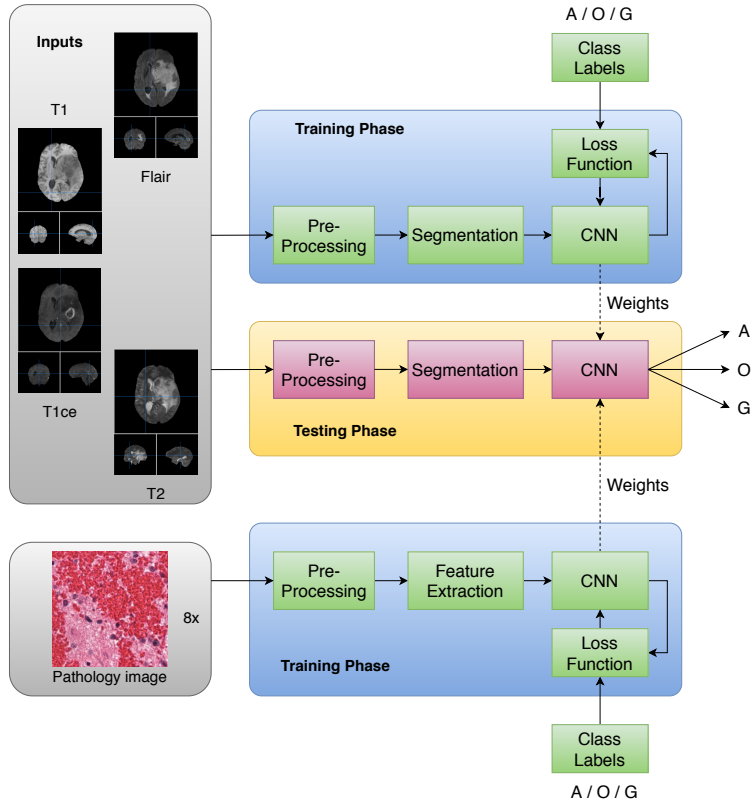


FIGURE 3.1: The flow diagram of the proposed model. Here, A - Astrocytoma, O - Oligodendrogloma and G - Glioblastoma

inputs. So, we crop the center part of the image and divided the cropped portion into several patches of 512x512. Then, the selected images are cropped again from dimensions 512x512 to 224x224. Random horizontal flips are performed on images during the training phase.

3.2 Segmentation

The segmentation algorithm proposed by Andriy has been used to segment the tumor from the MRI images [21]. The segmentation algorithm has been trained on BraTS 2019 dataset [16, 18, 19]. The trained model is used to segment on the CPM-RadPath 2019 dataset [20]. The dice-coefficient score achieved for the segmentation of the tumor has been 60.23%. The original MRI modalities are resized from the dimensions (240x240x155) to (80x96x64) and then these images are used as inputs for classification.

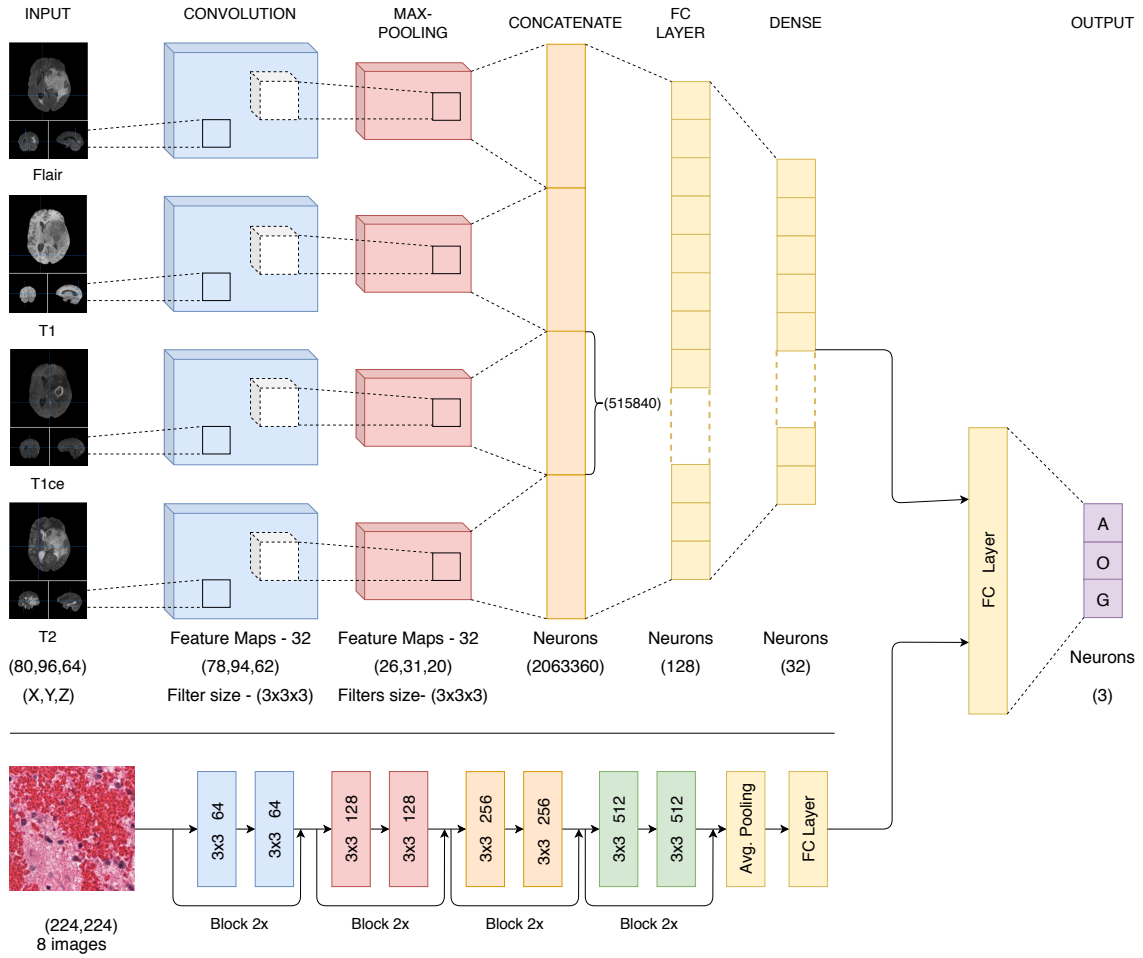


FIGURE 3.2: The proposed 3D convolutional neural network(CNN) architecture where the input layers consists of t1, t2, t1ce and flair images along with pathological images and the output layer consists of 3 neurons for each target class - Astrocytoma, Oligodendrogloma and Glioblastoma.

3.3 Convolutional Neural Network

Recently, convolutional neural networks(CNN) and it's variants has outperformed many classification algorithms [6, 11, 12]. The proposed model is a dual-path convolutional neural network for glioma classification namely, Astrocytoma, Oligodendrogloma and, Glioblastoma. The architecture of the proposed model is pictorially represented in the Figure 3.2

Four MRI modalities namely, T1-weighted(T1), post-contrast T1-weighted(T1ce), T2-weighted(T-2) and, T2-Fluid Attenuated Inversion Recovery(FLAIR) with the resized dimensions (80x96x64) have been given as input to the 3D CNN, in a parallel way as

shown in fig. 3.2. The CNN has 32 feature maps obtained by applying a 3x3x3 filter on each input modality with the stride of 1. The output of the convolutional layer is of the size (78x94x62). This has been given as input to a max-pooling layer obtained by applying a 3x3x3 filter on each input modality with the stride of 3. The output consists of 32 feature maps each of size (26x31x20).

The max-pooling layer captures the significant voxel which reduces the computational time. The output of the max-pooling layer has been concatenated into a 1D vector of neurons 5,15,840 for each modality. The total number of concatenated neurons are 20,63,360. This has been followed by three fully connected layers, each consisting of 128, 32 and 3 neurons respectively. The last layer gives a probability value ranging from 0 to 1 for each class. The neuron with the highest value has been considered as the tumor class. Rectified linear unit(ReLU) is used as an activation function, while the softmax activation function has been used in the last layer.

The pathological images are given as input to the model which is developed based on ResNet18 architecture. The input images are of dimensions 224x224. A block containing a convolutional 2D layer and a batch normalization 2D layer, which is repeated many times as necessary changing the parameters, thus achieving better results. The model takes in both segmented MRI images and pathological images as input for each patient. For each segmented MRI image, we pick the top eight patches from the pathological images of that patient that go into the same batch during training. If the patient has less than 8 pathology images, images are randomly picked selected for replacement. At the end of the 2D part of the combined model is an average operation that averages the features of the 8 images into one layer that is then concatenated into the 3D model as shown in the Figure 3.2. Hyper-parameters for the 3D CNN is given in table 3.1.

Stage	Hyperparameter	Value
Initialization	bias	zeros
	weights	Xavier uniform
SGD	alpha	0.01
Dropout	MRI-model	0.5
	Path-model	0.1
Training	epochs	20
	batch-size	8

TABLE 3.1: Caption

Chapter 4

Experimental Results

4.1 Dataset

The proposed model has been trained and validated on Computation Precision Medicine Radiology - Pathology 2019 (CPM-RadPath) dataset [20]. It consists three classes namely,

- Lower grade astrocytoma, IDH-mutant (Grade II or III).
- Oligodendrolioma, IDH-mutant, 1p/19q codeleted (Grade II or III).
- Glioblastoma and Diffuse astrocytic glioma with molecular features of glioblastoma, IDH-wildtype (Grade IV).

The dataset has radiology and pathology data of 221 patients as training data and 35 patient's data as validation data. Each patient has a T1, T1ce, T2, and, FLAIR MRI modalities 4.1, along with pathology images which are digitized whole slide tissue images captured from Hematoxylin and Eosin (H&E) stained tissue specimens. These tissue specimens are scanned at 20x and 40x magnifications.

All the images have been obtained from different institutions across the world, with different image acquisition protocols and scanners. The images have been pre-processed by co-registration to the same anatomical template which is then interpreted to the same resolution of ($1mm^3$), with skull-stripped.

The dataset consists of 133 patient's information suffering from glioblastoma, 54 from astrocytoma, and 34 from oligodendrolioma. So, additional care is necessary to handle this class imbalance issue.

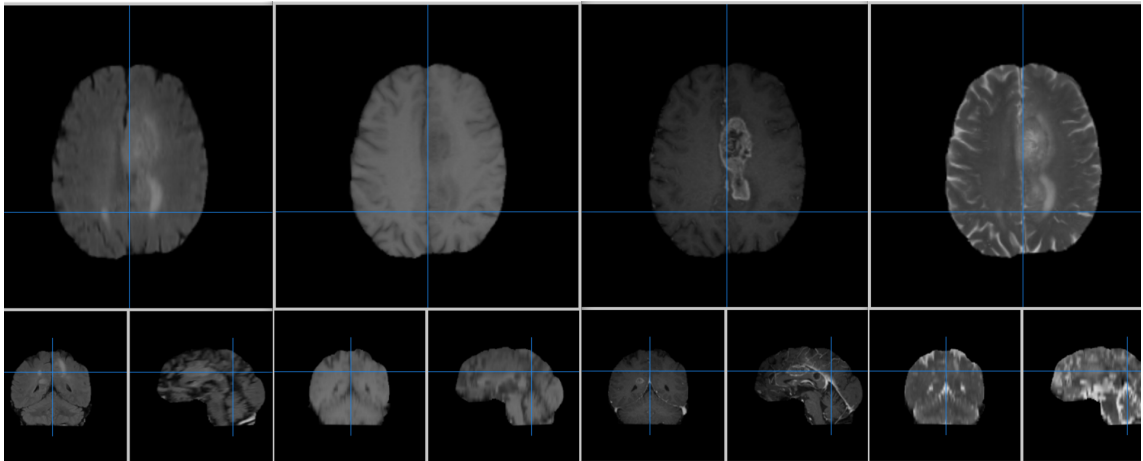


FIGURE 4.1: MRI modalities, i)FLAIR, ii)T1, iii)T1ce, and iv)T2

Figure 4.1 shows the four different modalities of a particular patient, each modality is a 3D image of dimensions 240x240x150. It is clear from the image that T1ce has better details about the necrosis region which helps in identifying the glioblastoma efficiently. The pathological images are present in the tilled tiff format, which is an efficient way of storing high resolution data. The given input .tiff image is cropped into several patches as shown in the Figure 4.2 which later are used to train the model. The dimensions of each cropped patch is 512x512.

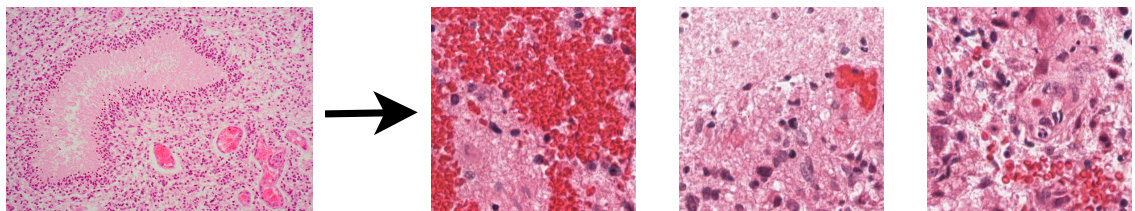


FIGURE 4.2: Few patches cropped from the brain tissue image.

4.2 Work Done and Results

4.2.1 Segmentation

To achieve better segmentation on the MRI images, we tried to maximize the crop size to 80*96*64 but had compromise on the batch size to 1 to be able to fit the network into GPU memory limits. The encoder and decoder both used the ResNet blocks, with two convolutions with batch normalization and ReLu activation function, followed by additive identity skip connection.

The loss function consists of 3 terms -

$$L = L_{dice} + 0.1 * L_{L2} + 0.1 * L_{KL}$$

L_{dice} is a soft dice loss applied to the decoder output p_{pred} to match the segmented mask p_{true} :

$$L_{dice} = \frac{2 * \sum p_{true} * p_{pred}}{\sum p_{true}^2 + \sum p_{pred}^2 + \epsilon}$$

L_{L2} is an L2 loss on the VAE branch output I_{pred} to match the input image I_{input} :

$$L_{L2} = \|I_{input} - I_{pred}\|_2^2$$

L_{KL} is standard VAE penalty term, a KL divergence between normal distribution and prior distribution and represented as:

$$L_{KL} = \frac{1}{N} \sum \mu^2 + \sigma^2 - \log \sigma^2 - 1$$

Adam optimizer with initial learning rate $\alpha_0 = 1e^{-4}$ and progressively decrease it according to:

$$\alpha = \alpha_0 * (1 - \frac{e}{N_e})^{0.9}$$

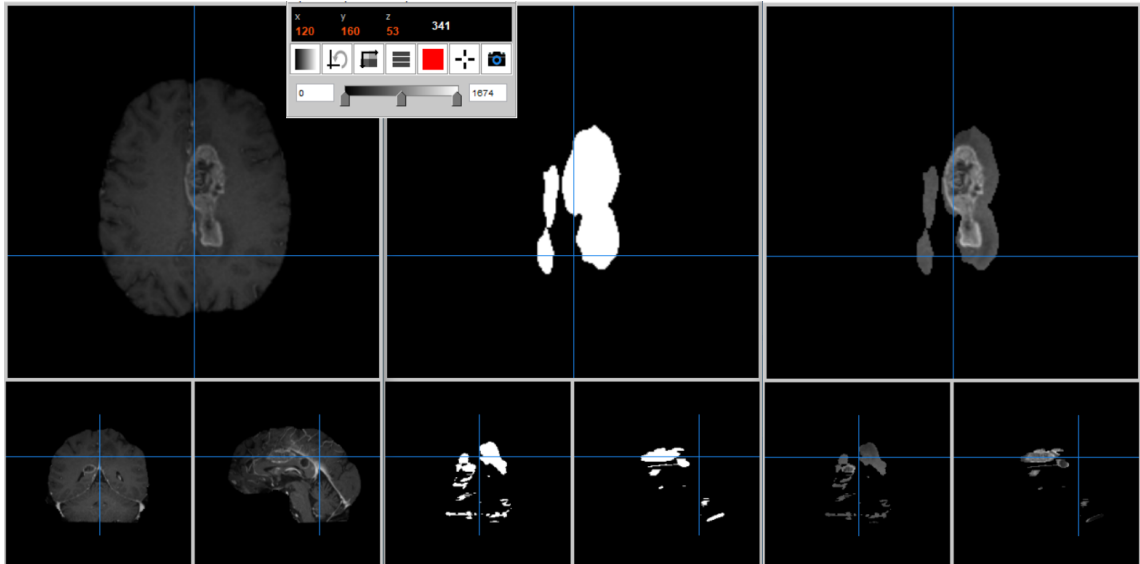


FIGURE 4.3: The tumor was segmented with a dice-coefficient of 0.6023

Figure 4.3 shows that the model was successful in segmenting the image yet retaining the most important regions of the tumor and achieved a dice-coefficient of 0.6023. We used this

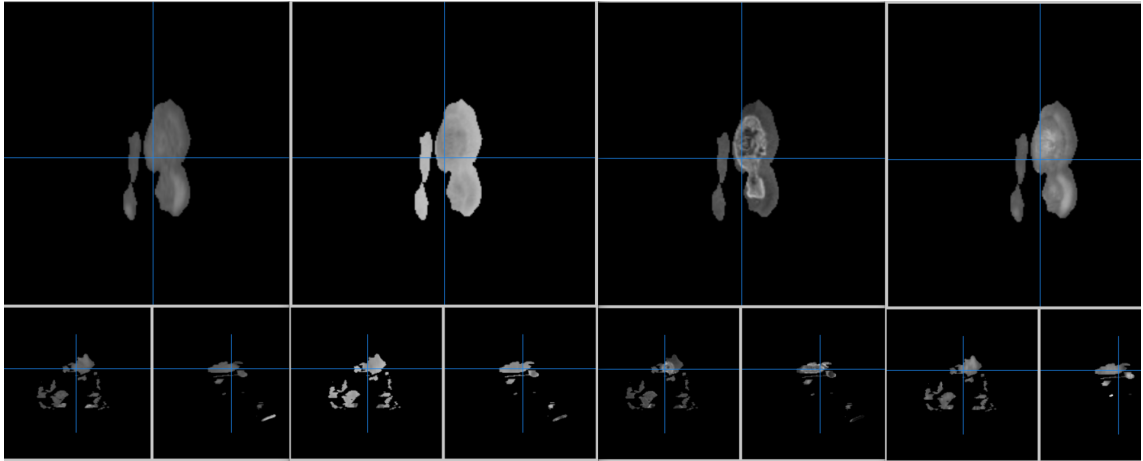


FIGURE 4.4: All the four modalities mask with the segmented tumor region.

segmented tumor output to mask the 4 modalities as shown in Figure 4.4, as the masked segmented images retain more information and thus achieve better classification accuracy.

Table 4.1 shows the difference in the accuracy when the model is trained on the MRI modalities when masked with the segmented tumor and when the model is trained on the whole MRI modalities along with the segmented tumor image.

Model	Input	Accuracy
Conv3D	t1ce, seg	0.6341
	masked(t1ce)	0.65
	flair, t1, t1ce, t2, seg	0.713
	masked(flair, t1, t1ce, t2)	0.7468

TABLE 4.1: Importance of masked segmented MRI images.

4.2.2 3-Class Classification on MRI images

The experiment has been studied on 2D and 3D Convolutional Neural Networks. The model has been trained and validated on T1ce MRI images alone, and also the study has been done by training the model on all the four MRI modalities(FLAIR, T1, T1ce, and T2). The experiment has been repeated with segmented and non-segmented MRI images as inputs. The model architecture is explained in the Figure 4.5.

We use, Adaptive Moment Estimation also known as Adam Optimizer, which is an efficient algorithm for optimizing an objective function. The adam's update rule is given as,

$$\theta_{t+1} = \theta_t - \frac{\eta}{\sqrt{\hat{v}_t + \epsilon}} \hat{m}_t$$

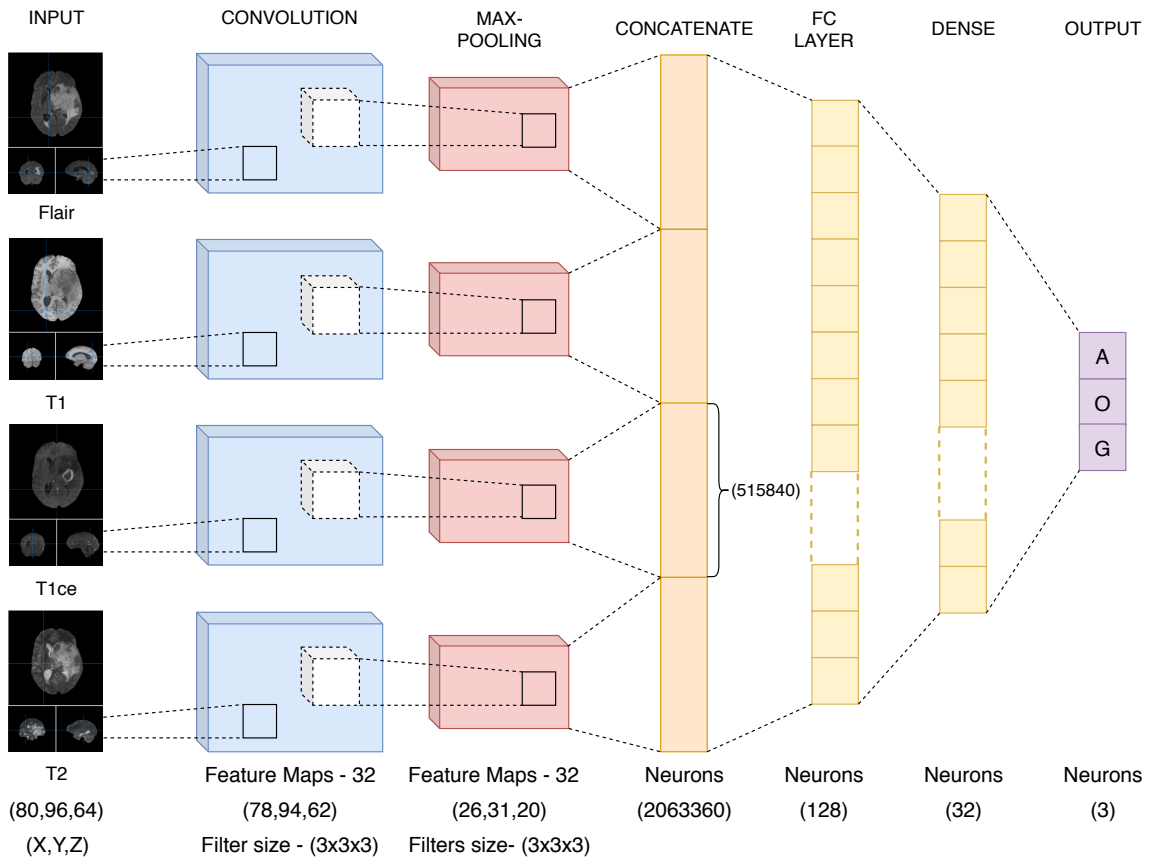


FIGURE 4.5: The proposed 3D convolutional neural network(CNN) architecture where the input layers consists of t1, t2, t1ce and flair images and the output layer consists of 3 neurons for each target class - Astrocytoma, Oligodendrogloma and Glioblastoma.

This is defined as the signal-to-noise ratio(SNR). The initialization bias-correction, especially during the initial time steps, and especially when the decay rates are very small, and using the relation,

$$v_t = (1 - \beta_2) \sum_{i=1}^t \beta_2^{t-i} \cdot g_i^2$$

Sparse categorical cross-entropy(SpCCE) is used as the classes are mutually exclusive, the formula for categorical cross-entropy(CCE) is given as,

$$CCE = -\frac{1}{N} \sum_{s \in S} \sum_{c \in C} 1_{s \in c} \log p(s \in c)$$

Since, the classes are mutually exclusive, we can modify the equation as,

$$SpCCE = -\log p(s \in c)$$

The training of the model has been done for 20 epochs with a batch size of 10 and Xavier uniform weights initialization. The accuracy is displayed in the Figure 4.6 for the model trained on segmented and non-segmented MRI images. The model trained with segmented MRI images as input achieved an accuracy of 74.68% and the model trained on whole MRI images got an accuracy of 63.15%. The model with only segmented T1ce modality as input was 65% accurate. It has been observed that the 3D CNN outperformed the 2D CNN, indicating that temporal information probably plays a role in classification accuracy.

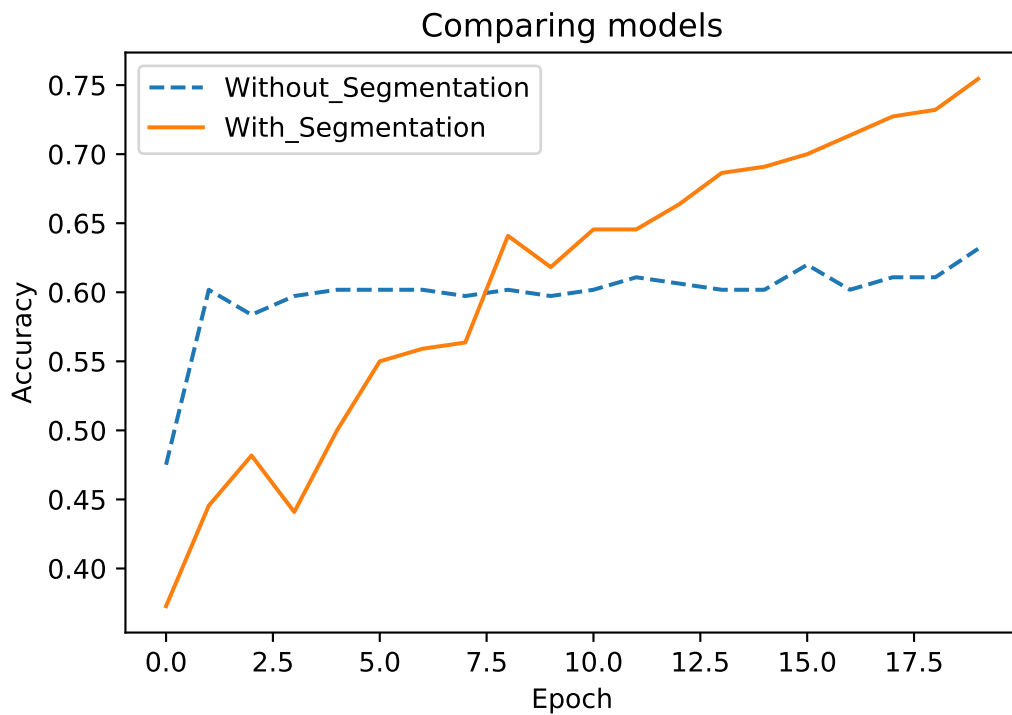


FIGURE 4.6: Accuracy of the proposed model on segmented and non-segmented MRI modalities(T1, T2, T1ce and FLAIR)

4.2.3 Binary Classification on MRI images

There is an evidence in the literature that Glioblastoma can be non-invasively diagnosed from T1ce MRI images(ring patterns) compared to other nodalities [14]. So, all T1ce MRI images of the CPM-RadPath dataset has been split into two classes namely, Glioblastoma and Non-Glioblastoma. The results obtained for this two class problem is shown in table 4.2. Cross validation has been performed by taking 15 Glioblastoma, 7 Oligodendrogloma and 8 Astrocytoma for validation and the remaining T1ce images are used for training. The cross validation is repeated 8 more times such that all Glioblastoma has been validated at least once and, the T1ce images used for validation is not present in the training set.

	T1ce				4 Modalities			
	Without Segmentation		With Segmentation		Without Segmentation		With Segmentation	
	G	NG	G	NG	G	NG	G	NG
G	114	13	120	14	113	11	121	12
NG	21	122	15	121	22	124	14	123
Accuracy	87.40%		89.25%		87.77%		90.3%	
F1-score	0.869		0.891		0.872		0.901	

TABLE 4.2: Confusion Matrix for Glioblastoma vs Non-Glioblastoma, with and without segmentation

From the results shown in table 4.2, it can be concluded that T1ce with the segmented tumor region can classify Glioblastoma accurately.

We conjecture that tumor position and size play a bigger role in tumor type than the entire MRI image. The segmentation model proposed by Andriy has been trained on BraTS 2019 [10] dataset and then this model is used to segment the MRI images from the CPM-RadPath dataset [20]. Thus we consider these segmented images as inputs to the model vs. the original MRI images. Combining the segmented MRI images with the pathological images under center crop gives a better accuracy of 77.73% as shown in the Table 4.3.

Neural Network Model	Input	Accuracy	Segmentation
ANN	t1ce	0.51	yes
ANN	flair, t1, t1ce, t2	0.60	yes
Conv2D	t1ce	0.625	yes
Conv2D	flair, t1, t1ce, t2	0.6544	yes
Conv3D	t1ce	0.6222	no
Conv3D	t1ce	0.65	yes
Conv3D	flair, t1, t1ce, t2	0.6315	no
Conv3D	flair, t1, t1ce, t2	0.7468	yes
ResNet 18	Pathology Images	0.6627	-
Dual-Path (Proposed)	flair, t1, t1ce, t2 & Pathology images	0.7773	yes

TABLE 4.3: Validation accuracy from various models with different inputs

Chapter 5

Conclusion

The proposed dual-path convolutional neural network has been tested on CPM-RadPath 2019 dataset on segmented MRI and pathological images. It has been observed that segmented input MRI images gave better results(74.68%) when compared to MRI images without segmentation(63.15%). Also there is evidence that 3D Convolutional Neural Network with temporal information about the glioma performs better than 2D Convolutional Neural Network with only neighbourhood information. Furthermore, the usage of additional MRI modalities (T1, T1ce, T2, and FLAIR) improved the accuracy when compared with both 3D and 2D CNN trained on single modality. The model trained on pathological images what were center cropped achieved an accuracy of 66.27%. So, pathological images alone cannot be good enough for classification, so we developed a dual-path convolutional neural network which takes both the segmented MRI images along with the pathological images to obtain a higher classification accuracy which is 77.73%. Also, the proposed model has been tested for Glioblastoma and Non-Glioblastoma (Astrocytoma and Oligodendroglioma) with T1ce images alone. For the 2-class problem, an accuracy of 89.2% has been obtained which shows that Glioblastoma can be identified non-invasively from T1ce MRI images.

Bibliography

- [1] M. A. Charlton-Perkins, E. D. Sendler, and et al., “Multifunctional glial support by semper cells in the drosophila retina,” *PLos genetics*, vol. 13, no. 5, 2017.
- [2] N. J. Allen and B. A. Barres, “Gliamore than just brain glue,” *Nature*, vol. 457, no. 7230, pp. 675–677, 2009.
- [3] Q. T. Ostrom, H. Gittleman, and et al., “Cbrtrus statistical report: Primary brain and other central nervous system tumors diagnosed in the united states in 2009–2013,” *Neuro-Oncology*, vol. 18, no. 5, pp. 1–75, 2016.
- [4] D. N. Louis, A. Perry, and et al., “The 2016 world health organisation classification of tumors of the central nervous system: a summary,” *Acta neuropathologica*, vol. 131, no. 6, pp. 803–820, 2016.
- [5] S. Pereira, A. Pinto, and et al., “Brain tumor segmentation using convolutional neural networks in mri images,” *IEEE Transactions on Medical Imaging*, vol. 35, no. 5, pp. 1240–1251, 2016.
- [6] G. C, G. IY, and et al., “Deep learning and multi-sensor fusion for glioma classification using multistream 2d convolutional networks,” *International Conference of the IEEE Engineering in Medicine and Biology Society (EMBC)*, vol. 40, no. 8, pp. 5894—5897, 2018.
- [7] M. Prastawa and et al., “A brain tumor segmentation framework based on outlier detection,” *Medical Image Analysis*, vol. 8, no. 3, pp. 275—283, 2004.
- [8] D. Zikic and et al., “Segmentation of brain tumor tissues with convolutional neural networks,” *MICCAI BraTS Challenge*, pp. 36—39, 2014.
- [9] V. Rao, M. Sharifi, and et al., “A brain tumor segmentation framework based on outlier detection,” *MICcAI BraTS Challenge*, pp. 56—59, 2015.

- [10] B. Menze and et al., “The multimodal brain tumor image segmentation benchmark (brats),” *IEEE Transaction on Medical Imaging*, vol. 34, no. 10, pp. 1993—2024, 2015.
- [11] M. Sajjad, S. Khan, and et al., “Multi-grade brain tumor classification using deep cnn with extensive data augmentation,” *Journal of Computational Science*, vol. 30, pp. 174–182, 2019.
- [12] J. Cheng, W. Huang, and et al., “Enhanced performance of brain tumor classification via tumor region augmentation and partition,” *PloS one*, vol. 10, no. 10, 2015.
- [13] P. Afshar, A. Mohammadi, and et al., “Brain tumor type classification via capsule networks,” *International Conference on Image Processing(ICIP)*, pp. 3129–3133, 2018.
- [14] C. Ge, “Cross-modality augmentation of brain mr images using a novel pairwise generative adversarial network for enhanced glioma classification,” *International Conference on Image Processing(ICIP)*, pp. 559–563, 2019.
- [15] S. Bakas, H. Akbari, and et al., “Advancing the cancer genome atlas glioma mri collections with expert segmentation labels and randomic features,” *Scientific data*, vol. 4, 2017.
- [16] B. Erickson, Z. Akkus, and et al., “Data from 1gg-1p19qdeletion,” *The Cancer Imaging Archive*, 2017.
- [17] S. Liu, Y. Wang, and et al., “Relationship between necrotic patterns in glioblastoma and patient survival: fractal dimension and lacunarity analyses using magnetic resonance imaging,” *Scientific Reports*, vol. 7, 2017.
- [18] C. Houillier, X. Wang, and et al., “Idh1 or idh2 mutations predict longer survival and response to temozolomide in low-grade gliomas,” *Neurology*, vol. 75, no. 17, pp. 1560–1566, 2010.
- [19] H. Yan, W. Parsons, and et al., “Idh1 and idh2mutations in gliomas,” *New England Journal of Medicine*, vol. 360, pp. 765–773, 2009.
- [20] H. Yan, “Computational precision medicine: Radiology-pathology challenge on brain tumor classification 2019 (cpm-radpath),” *Miccai Conference 2019*, 2019.
- [21] A. Myronenko, “3d mri brain tumor segmentation using autoencoder regularization,” *BrainLes 2018*, vol. 11384, 2018.